Morphological Changes from Silica Tubules to Hollow Spheres Controlled by the Intermolecular Interactions within Block Copolymer Micelle Templates

Hyemin Lee[†] and Kookheon Char*

School of Chemical and Biological Engineering, Interdisciplinary Program in Nano-Science & Technology, and Center for Functional Polymer Thin Films, Seoul National University, San 56-1, Shilim-dong, Kwanak-gu, Seoul 151-744, Korea

ABSTRACT The morphological changes from tubules to large hollow spheres to (micelle-sized) small hollow-spherical silica were realized by polystyrene-*block*-poly(vinylpyridine) (PS-*b*-PVP) block copolymer micelle templates by controlling the intermolecular interactions with the corona chains. PS-*b*-PVP with weak intermolecular interactions among PVP corona chains yields the coexistence of tubules, large hollow spheres, and small hollow spheres. The coexistence of the three phases arises from the direct aggregation of block copolymer micelles during hydrolytic condensation of a silica precursor (tetraethylorthosilicate), as evidenced by transmission electron microscopy. When the degree of intermolecular interactions within the PVP corona blocks is increased by a change in either the degree of quaternization of the PVP blocks or the dielectric constant of the medium, small hollow spherical silica, with size equivalent to the block copolymer micelles, were solely obtained. We believe that this morphological change is due to the fact that the dipole−dipole interactions among quaternized PVP blocks physically cross-link the PVP coronas in micelles resisting the curvature change during the silica condensation.

KEYWORDS: hollow silica • block copolymer micelle(s) • quaternization • dielectric constant • intermolecular interaction(s)

1. INTRODUCTION

Hollow materials have been investigated for many potential uses in storage, carriers for drugs (1), catalysis (2), and supports for enzyme immobilization and encapsulation (3). Furthermore, other interesting applications can also be suggested depending on the chemical composition of the hollow shells, size, and morphology of the hollow objects. Silica is well-known to be thermally and chemically stable such that it can be one of the excellent candidates protecting active ingredients against the external environment (1, 4).

Various synthetic methods to prepare hollow silica have recently been introduced. Emulsion systems (5), spray drying (6), and layer-by-layer deposition on colloidal templates (7) have been attractive for the preparation of hollow spheres with a variety of inorganic shells. However, they all have difficulty in preparing nanosized hollow shells, and thus this disadvantage limits their applications in nanotechnology. Block copolymer micelle templates, which have recently been introduced, are easily control the size and morphology of hollow particles in a nanometer scale. Amphiphilic block copolymers containing both hydrophilic and hydrophobic blocks can readily self-assemble into nanosized micelles with various morphologies above the critical micelle concentration in a selective polar solvent. Recently, hollow silica spheres with size less than 50 nm have been prepared with block copolymer templates. If block copolymer micelles, formed in a selective solvent, are stable enough to maintain their size and shape during the hydrolytic condensation of silica precursors, hollow silica with size equivalent to that of the micelles can be obtained. For example, Nakashima and co-workers demonstrated hollow silica nanospheres with diameter of 30 nm and a void space of 11 nm, which are attributed to the size of the micelles of a triblock copolymer (PS-*b*-PVP-*b*-PEO) (8a). Also, Armes and co-workers reported the spherical block copolymer micelle/silica hybrids obtained from nanosized cationic diblock copolymer micelles (PDPA-*b*-PDMA) (8b). With a silica shell synthesized in the corona region of the micelles, these hybrids have high stability against the condition where dissociation in the micelles would occur. Those hollow silica spheres are uniform in size, originating from the size of the micelles.

When an inorganic precursor associates with an amphiphilic organic template such as surfactants and block copolymers, the importance of counterions for charged templates has been demonstrated to control the physical properties of the final hierarchical organization. The general synthetic route to form interfaces between organic and inorganic materials involves the mediated association of cationic inorganic materials (I^+) with cationic templates (S^+) under acidic condition ($S^+X^-I^+$). In this case, the counterion

* Corresponding author. Tel: +82-2-880-7431. Fax: +82-2-873-1548. E-mail: khchar@plaza.snu.ac.kr.
Received for review January 12, 2009 and accepted March 16, 2009
† E-mail: hm928@snu.ac.kr.
DOI: 10.1021/am900026s

(X^-), as a mediator, plays an important role in balancing the charge and, at the same time, in controlling the interfacial curvature of organic/inorganic hybrids (9). This, in turn, implies that the strength of the ion binding of counterions to charged templates has an enormous influence on the final morphology, providing highly ordered structure in mesoporous silica depending on the type of counterion species employed (10).

The strength of the counterion binding to charged templates can also be controlled by the composition of the medium. This phenomenon has its origin in Coulomb's law (11). If there are two electric charges (with q_1 and q_2), they interact with each other through the electrostatic Coulombic force: like charges repel each other, while unlike charges attract each other. The magnitude of the Coulombic force is given as follows:

$$F = k_e \frac{q_1 q_2}{r^2} = \frac{1}{4\pi\epsilon} \frac{q_1 q_2}{r^2} \quad (1)$$

where r is the distance between the two charges (q_1 and q_2), k_e is the Coulombic force constant, and ϵ is the dielectric constant. In our experiments, those two charges interact with each other in solution, and the dielectric constant of a medium, ϵ, can be applied to eq 1. That is to say that the attractive interaction between two opposite charges (i.e., the interaction between positively charged PVP blocks and negatively charged counterions such as Cl^- and I^- in the present case) can be controlled by the dielectric constant of the medium which, in turn, can be varied by the composition in the mixed medium. The concept for controlling the Coulombic interactions through a change in the dielectric constant of the mixed medium has already been applied to the collapse/swelling behavior of polymer gels through the formation of multiple ion pairs (12).

Here, we report the morphological change of nanosized hollow silica from tubules to spheres based on block copolymer micelles. In addition, we elucidate the origin of such morphological change based on the quarternization (or the number of ion pairs) of PVP blocks as well as the change in the dielectric constant of the mixed medium (i.e., ethanol/water mixed solvent). Unlike surfactants with single polar head groups, charged block copolymer templates have plenty of connected charge groups. Two experimental parameters (the number of tightly bound ion pairs and the dielectric constant of the mixed medium) control the electrostatic attraction between charged corona chains and their counterions. Moreover, the intermolecular interaction within the corona chains through the dipole−dipole interactions has a significant effect on the interfacial curvature during the association and condensation of silica precursors.

2. EXPERIMENTAL DETAILS

Synthesis of Poly(styrene-*block*-4-vinylpyridine) (PS-*b*-P4VP). PS-*b*-P4VP block copolymer was synthesized by anionic polymerization (13). The sequential polymerization of styrene (Aldrich) and 4-vinylpyridine (Aldrich) was carried out in an argon atmosphere. All of the monomers used were purified with CaH_2. *sec*-Butyllithium (Aldrich) was used as an initiator for the polymerization of styrene in tetrahydrofuran at −78 °C. Upon completion of PS polymerization, 4-vinylpyridine was added to the polymerization reactor. The reaction was terminated with degassed methanol. The block copolymer was obtained by precipitation in water and dried under vacuum at 60 °C for 2 days. The total molecular weight of PS-*b*-P4VP is 77K with PDI of 1.15, and the volume fraction of the PS block is 0.36.

Quaternization of PS-*b*-P4VP. PS-*b*-P4VP was quaternized in chloroform ($CHCl_3$) with methyl iodide (CH_3I) as a quaternizing agent (14). An excess of CH_3I was added to a 3 wt % solution of PS-*b*-P4VP block copolymer, and the quaternization reaction maintained the reaction temperature at 45 °C. The degree of quaternization (DQ) was controlled by the amount of quaternization agent as well as the reaction time. Quaternized PS-*b*-P4VPs (denoted as PS-*b*-QP4VP) were recovered by precipitation in hexane. The PS-*b*-QP4VP products were filtered and dried in a vacuum oven for 1 day.

Preparation of Hollow Silica. PS-*b*-P4VPs and PS-*b*-QP4VPs were first dissolved in $CHCl_3$. After solutions containing block copolymers became clear, $CHCl_3$ was removed under a gentle flow of nitrogen until the content of $CHCl_3$ in the solution remained below 1 wt %. An excess of ethanol was then added, and the resulting solution was vigorously stirred. The mixed solvent was removed using the same method as that used to remove $CHCl_3$. The process of solvent exchange was repeated more than three times. Block copolymers were initially dissolved in ethanol, and distilled water at pH 2, titrated with hydrogen chloride (HCl), was then slowly added to make up 5 wt % block copolymer solutions in the final mixed solvent (distilled water:ethanol = 4:1 by weight). After the solution was well stirred for 1 day, a given amount of tetraethylorthosilicate (TEOS), a silica source, was slowly dropped into a beaker containing the block copolymer solution. The molar ratio of 4-vinylpyridine [repeat unit of (Q)P4VP] with respect to TEOS was kept constant at 1:2.4. After the reaction mixture was stirred for 1 day at 25 °C, the silica products were aged for 2 days at 80 °C. Calcination was finally carried out in a furnace at 450 °C for 3 h.

For studies on the morphological change by variation of the weight ratio of ethanol in water/ethanol mixtures, the same amount of PS-*b*-P4VPs was dissolved in a mixed medium with X = 10, 20, 30, and 70 (by weight) in X:100 ethanol/water. In order to investigate the effect of the ethanol content on the morphology of hollow silica, the molar ratios of all of the reactants used except ethanol were fixed (i.e., 1:0.001:0.043:X:54.19 TEOS/PS-*b*-P4VP/HCl/ethanol/H_2O).

Preparation of Micelle Solutions for Transmission Electron Microscopy (TEM) Measurements. The preparation method was the same as that of a block copolymer micelle solution to produce hollow silica. First, a 5 wt % block copolymer solution was prepared using a mixture of 4:1 (wt %) H_2O (pH 2)/ethanol. The block copolymer solution was further diluted to 0.1 wt % with the same mixed solvent for examination with TEM. After the solution was stirred for 1 day, it was dropped on a carbon-coated grid, and the grid was dried overnight before examination with TEM. In order to obtain micelle morphology and to determine the micelle size, the block copolymer was stained by RuO_4. TEM measurements were performed on a JEOL JEM-2000EXII at a 200 kV electron beam accelerating voltage.

3. RESULTS AND DISCUSSION

Hollow silica with different morphologies were prepared by the sol−gel reaction with block copolymer micelles (PS-*b*-P4VP; total molecular weight of 77K with a volume fraction of the PS block of 0.36) in the presence of a silica precursor (TEOS; Scheme 1). PS-*b*-P4VP consists of a nonpolar PS block and a polar P4VP block. In order to realize the sol−gel reaction with TEOS precursors, PS-*b*-P4VP should first be soluble in the form of micelles in an aqueous solution, and

Scheme 1. Schematic Illustration of Hollow Silica with Different Morphologies Templated by Block Copolymer Micelles

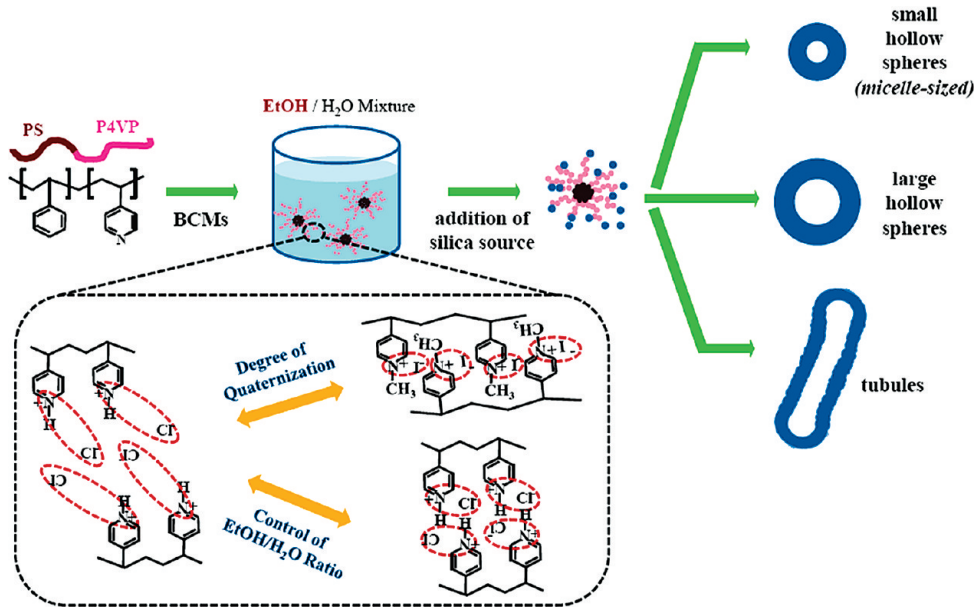

Table 1. Experimental Conditions for the Quaternization of PS-*b*-P4VP with a Quaternizing Agent (CH_3I)

sample	CH_3I amount (excess molar ratio)[a]	temperature [°C]	reaction time [h]	conversion [%]
B	65	45	1	5
C	95	45	2	10
D	60	45	4	20
E	125	45	16	30

[a] With respect to the molar content of P4VP in PS-*b*-P4VP (77K).

this requirement can be met at a pH lower than the pK_a value (~5.0 ± 0.3) (15) of the PVP block. It is also noted that block copolymer micelles can be soluble in an aqueous solution in the entire pH region by quaternization of the PVP blocks. Quaternization of the PVP blocks with different counterions could change the tightness of the dipoles, which, in turn, modulates the intermolecular interactions within the PVP corona chains in the micelles. For example, I^- ions were employed as counterions in the quaternization of PVP blocks, and the dipoles formed between the charged PVP and I^- counterions are tightly bound, thus controlling the intermolecular interactions among the PVP corona chains through dipole−dipole interactions. Furthermore, the intermolecular interactions among the PVP corona chains influence the resistance to interfacial curvature change upon condensation with silica precursors.

3.1. Effect of Quaternization. We prepared quaternized block copolymers (PS-*b*-QP4VPs) using a quaternizing agent, iodomethane (CH_3I) (14). Table 1 describes the experimental conditions for the quaternization of PVP blocks such as the amount of CH_3I, reaction time, and reaction temperature. Figure 1A shows that peak c, assigned to the pyridine ring, decreases while peaks c′ and d, originating from the quaternized pyridine ring and the covalent alkyl chains, increase upon quaternization. The DQ for each sample was estimated based on the ^{1}H NMR data (16). The molar ratio of the initial P4VP to PS blocks was estimated based on the integrated values of a signal a originating from the PS blocks, which are intact during the quaternization, and a signal c in PS-*b*-PVP (part A in Figure 1) before quaternization. The ratio of the integrated value of signal c′ to the initial integrated value of signal c for the PVP blocks is the DQ. We prepared PS-*b*-QP4VPs with different DQs (5%, 10%, 20%, and 30%, respectively), in which the numbers shown are the molar quaternization values of the PVP blocks.

When PS-*b*-P4VP and PS-*b*-QP4VPs are dissolved in a selective solvent (i.e., a mixture of ethanol and distilled water at pH = 2), the shapes of the micelles formed in

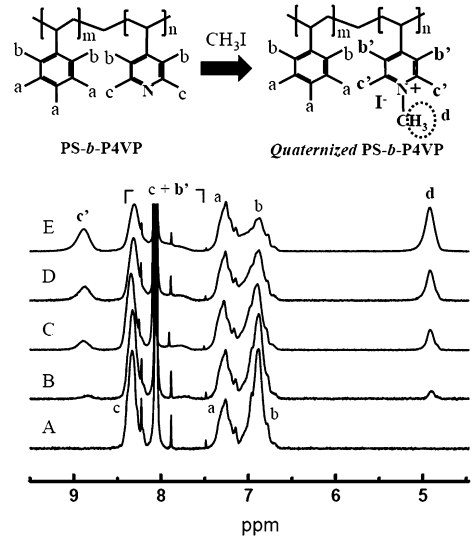

FIGURE 1. ^{1}H NMR spectra of PS-*b*-P4VP and quaternized PS-*b*-P4VPs: (A) PS-*b*-P4VP; (B) PS-*b*-QP4VP (5%); (C) PS-*b*-QP4VP (10%); (D) PS-*b*-QP4VP (20%), and (E) PS-*b*-QP4VP (30%) dissolved in deuterated dimethylformamide. Tetramethylsilane at a fixed concentration was used as the internal standard.

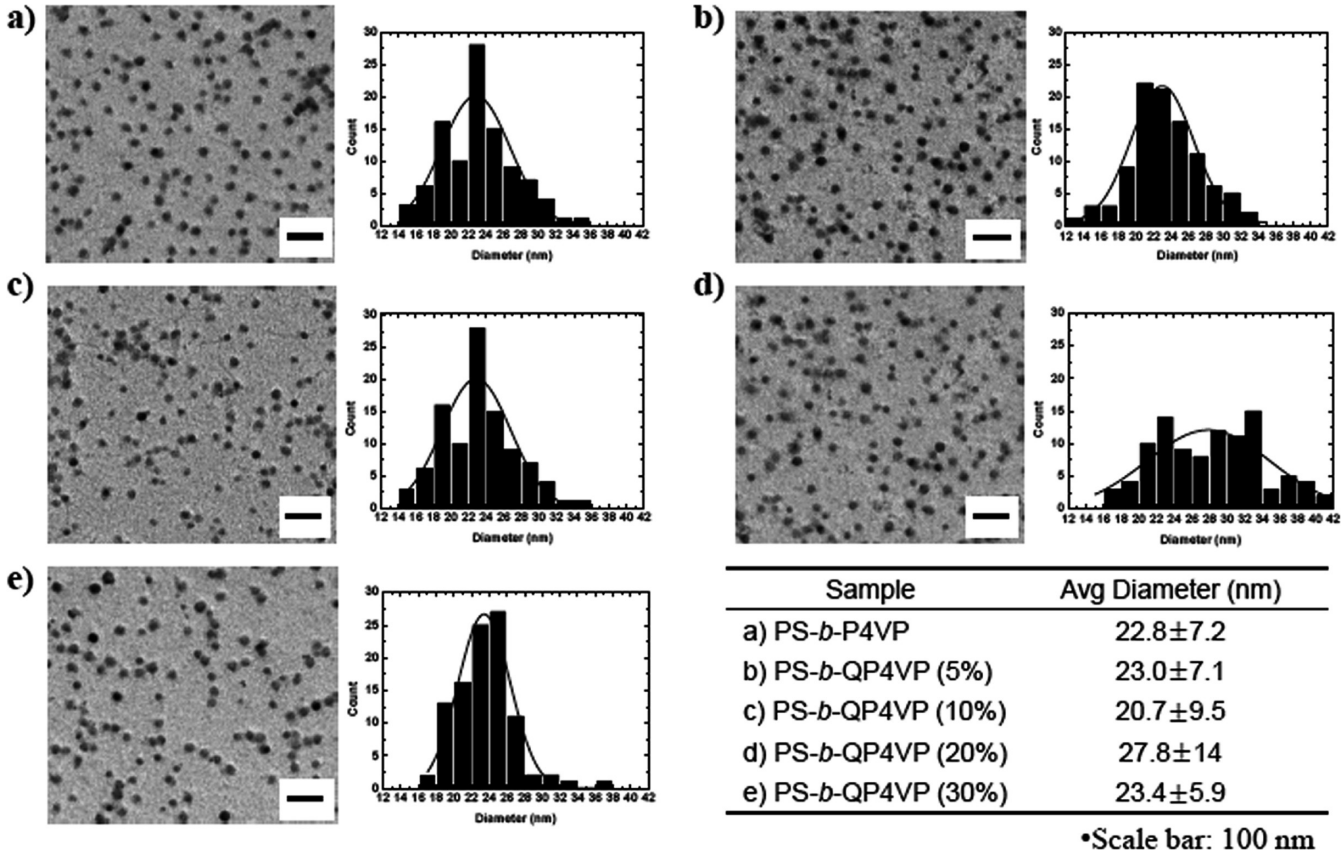

FIGURE 2. TEM images of spherical micelles and their size distribution: (a) PS-*b*-P4VP; (b) PS-*b*-QP4VP (5%); (c) PS-*b*-QP4VP (10%); (d) PS-*b*-QP4VP (20%), and (e) PS-*b*-QP4VP (30%) dissolved in a mixture of ethanol and distilled water at pH 2.

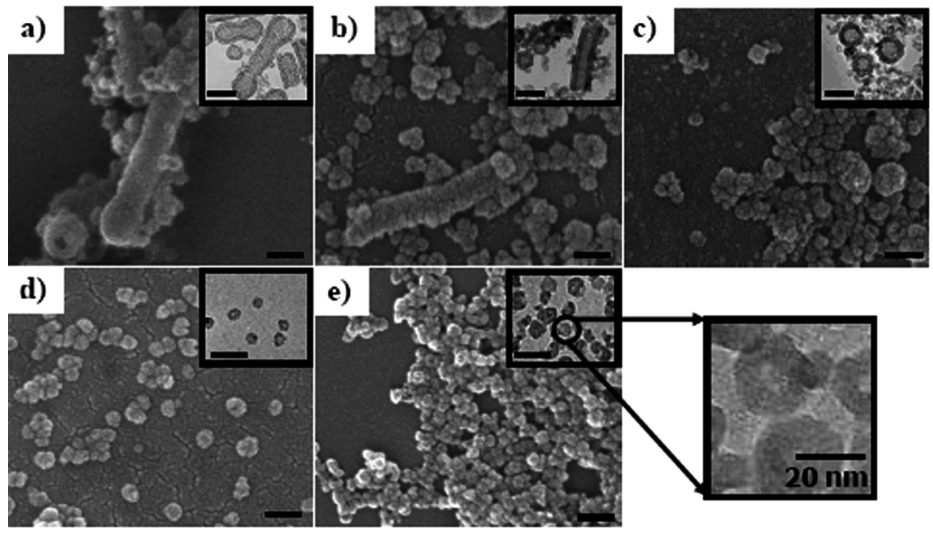

FIGURE 3. FE-SEM and TEM (inset) images of hollow silica obtained with various cationic block copolymer micelles with varying DQs: (a) PS-*b*-P4VP; (b) PS-*b*-QP4VP (5%); (c) PS-*b*-QP4VP (10%); (d) PS-*b*-QP4VP (20%); (e) PS-*b*-QP4VP (30%). All of the scale bars in the pictures are 100 nm.

such a selective solvent, with the PS blocks comprising the micelle cores and the QP4VP blocks located in coronas, are spherical irrespective of the DQ of PVP blocks, as shown in Figure 2.

Figure 3 shows the TEM (inset) and field-emission scanning electron microscopy (FE-SEM) images of hollow silica after calcination. We obtained a mixture of hollow tubules and (large and small) hollow spheres when the (unquaternized) PS-*b*-P4VP template was employed (Figure 3a). The diameter of the tubules ranging from 58 to 118 nm was much larger than the size of the PS-*b*-PVP micelles. We also note the undulating surfaces of the tubules, which lead us to think that the origin of such tubule formation might be from aggregation of the micelles. Hollow spheres coexist with the tubules in the size range from 21 to 109 nm. The silica shell thickness of the hollow tubules and spheres was about 8−19 nm, which is dependent on the size of the final hollow objects.

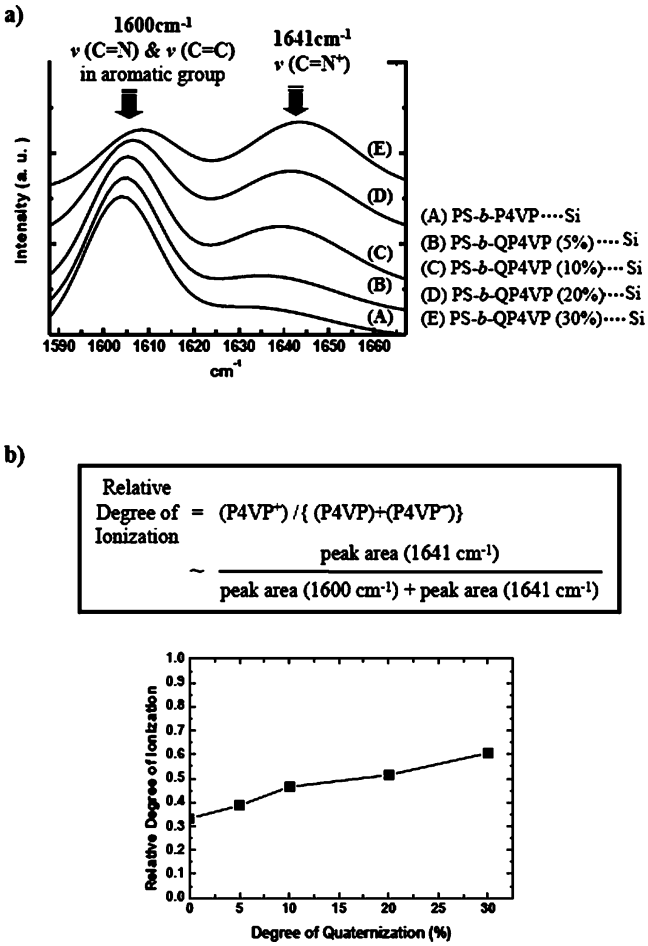

FIGURE 4. FT-IR spectra of micelle/silica hybrids showing that ionic groups, associated with a silica source, increase with an increase in the DQ. In the FT-IR spectra, the vibration peak around 1600 cm^{-1}, assigned to both C═C and C═N, decreases while the vibration peak at 1641 cm^{-1}, assigned to $C{=}N^+$ in $P4VP^+$, increases with higher conversion of quaternization. Because the PS blocks are intact during quaternization of the PVP blocks, the relative degree of ionization of the PVP blocks can be determined by deconvolution of these two peaks.

As the DQ of PS-*b*-P4VP is increased, the number of tubules and large hollow spheres above 55 nm in size drastically decreases, while the number of small hollow spheres with diameter of less than 55 nm increases (see Figure S1 in the Supporting Information). We also note that the number density of tubules decreases upon an increase in the quaternization of P4VP blocks, as evidenced in Figure 3b for PS-*b*-QPVP (5 mol % DQ). At the same time, the number density of large hollow spheres in the range of 55−111 nm increases. However, the size distribution of hollow spheres ranging from 21 to 111 nm still remains polydisperse when compared with the size distribution based on the PS-*b*-P4VP templates (see Figure 3a,b).

When the DQ is further increased to 10%, tubules are no longer observed and instead there is the coexistence of small (20−55 nm in size) and large (60−110 nm) hollow spheres with the dominant presence of small hollow silica, as shown in Figure 3c (see Figure S1 in the Supporting Information). Upon a further increase in the DQ of PS-*b*-P4VPs (20% and 30%), we only find small hollow silica with sizes ranging

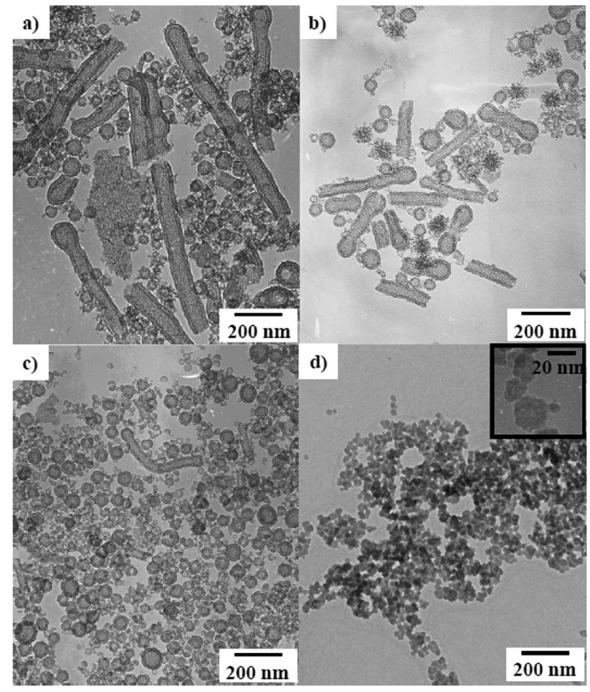

FIGURE 5. Hollow silica with different morphologies were synthesized using block copolymer micelle templates in a mixture of *X*:100 (wt %) ethanol/distilled water (pH 2). The increase in the ethanol content significantly affects the morphology of hollow silica: (a) $X = 10$; (b) $X = 20$; (c) $X = 30$; (d) $X = 70$.

from 20 to 55 nm, and the size distribution of such small hollow silica is fairly narrow.

The increase in the DQ implies the concurrent increase in the number of ion pairs (quaternized amines and associating I^- counterions) per P4VP block chain. We also note that the total concentration of ionic groups originating from the block templates increases with an increase in the DQ. This trend was confirmed by FT-IR spectra in micelle/silica hybrid compounds, as shown in Figure 4.

3.2. Effect of Ethanol. In the above experiments, it was demonstrated that hollow silica with different morphologies could be generated in a mixture of ethanol and water at pH 2. Ethanol enhances the solubility of TEOS as well as the solubility of PS-*b*-P4VP templates. Furthermore, the addition of ethanol ($\epsilon = 25$) reduces the dielectric constant in solution (17), which, in turn, enhances the stability of counterion binding (even with loosely bound Cl^-). In order to study the evolution of the hollow structure with different morphologies by the extent of counterion binding, the same amounts of PS-*b*-P4VP templates were dissolved in a mixture of ethanol and water (at pH 2) with $X = 10$, 20, 30, and 70 (by weight) in *X*:100 ethanol/water.

Figure 5 demonstrates that the morphological changes for the hollow silica show the same trend as the morphological changes with quaternized PS-*b*-P4VPs. The coexisting phase of tubules and (large and small) hollow spheres is observed in low ethanol content ($X = 10$ and 20). Long tubules observed at low ethanol content ($X = 10$), however, become shortened, and the diameter distribution in tubules becomes narrower with $X = 20$, as shown in Figures 5 and S2 (Supporting Information). As the ethanol content is

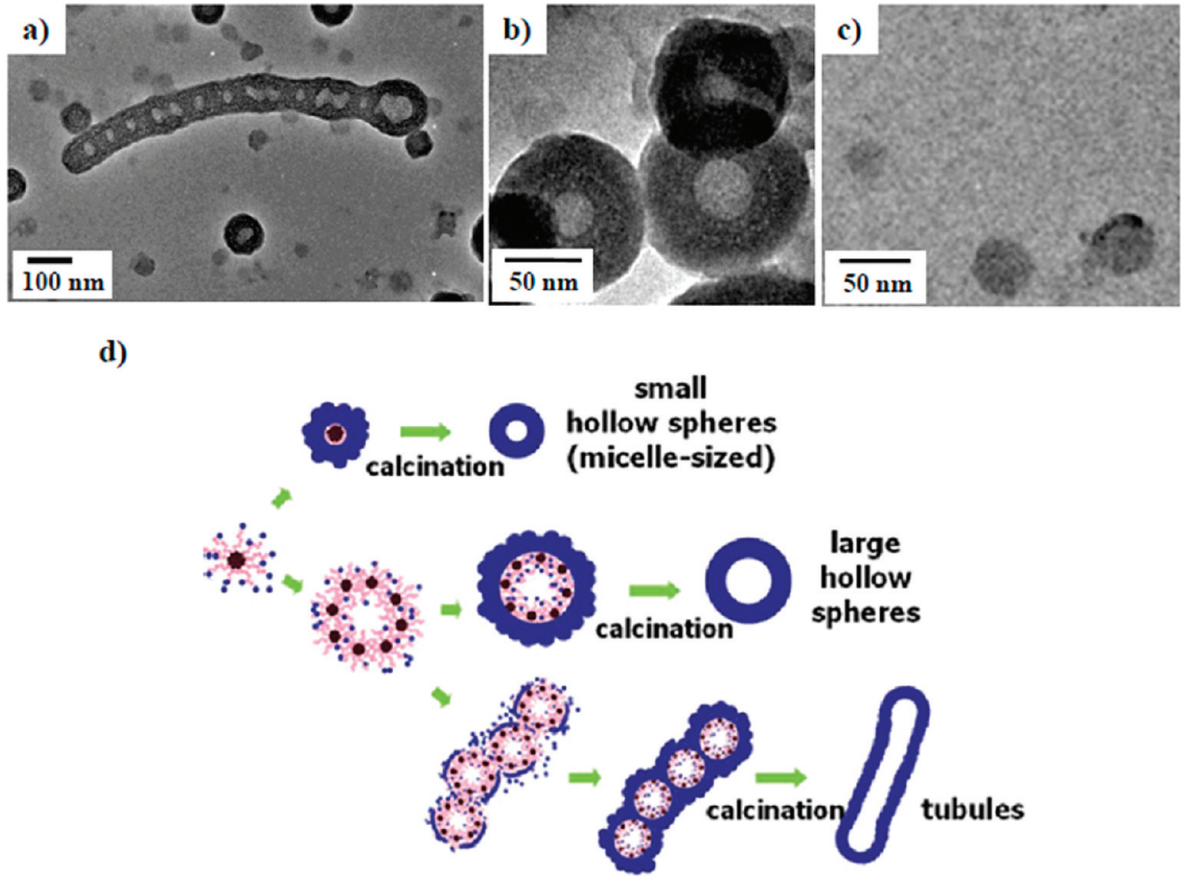

FIGURE 6. TEM images of as-synthesized silica with three different shapes templated by PS-*b*-P4VP: (a) Tubules connected with hollow spheres by directed aggregation. (b) Hollow spheres with diameter of above 55 nm formed by aggregation of elementary micelle/silica hybrids. (c) Hollow spheres with diameter of below 55 nm formed by direct micelles. (d) Schematic illustration of the formation mechanism of tubular and spherical hollow silica, which is demonstrated by TEM images (a–c).

increased up to $X = 30$, the fractions for hollow spheres are dominant and only a few tubules are observed. Upon a further increase in the ethanol content ($X = 70$), only small hollow spheres with diameter of less than 50 nm are observed under TEM and the size distribution of small hollow spheres becomes narrow as in the case for small hollow spheres with highly quaternized PS-*b*-QP4VP (with 20% and 30% of DQ).

3.3. Mechanism of Hollow Silica. ***3.3.1. Effect of Quaternization.*** Counterion effects on the self-assembly of surfactants have been referred to in the Hofmeister series of anions (18). The anions were initially classified as the degree of impact on the protein solubility in an electrolyte solution. Typically, the Hofmeister series order anions in enhancing the protein solubility as follows: $SO_4^{2-} < HPO_4^{2-} < OH^- < F^- < HCOO^- < CH_3COO^- < Cl^- < Br^- < NO^{3-} < I^- < SCN^- < ClO^{4-}$. Anions on the left side of Cl^- are small in size with relatively low polarizability and thus become hydrated easily. However, anions on the right side of Cl^- with large size possess high polarizability and reduce the degree of water hydration, leading to the formation of strong ion pairs.

According to the Hofmeister series, I^- counterions lead to the strong ion pairs in quaternized P4VP blocks. The tight interaction between quaternized amines and I^- counterions significantly influences the final structure of hollow silica. The strong dipole–dipole interactions between tightly bound ion pairs physically cross-link the corona region (12b), keeping the micelles from deformation or morphological change during association with silica precursors. At the same time, I^- is also known to readily link between quaternized amine and positively charged silica in acidic conditions, and thus the tightly bound I^- accelerates the condensation of silica precursor near the quaternized P4VP blocks (10a). We believe that the small hollow silica that we observe with PS-*b*-QP4VP templates with DQ higher than 20% are derived from the micelles of size of around 25 nm.

On the other hand, when block templates with DQ lower than 10% are used, the coexistence among tubules and large/small hollow spheres is observed. We also note that the diameter of the tubules and large hollow spheres is much larger than the elementary micelle size. In order to find clues for hollow objects with larger size, we investigated the morphology of as-synthesized micelle/silica hybrid compounds templated with PS-*b*-P4VP (Figure 6). As-synthesized samples were stained by RuO_4, staining both PS and P4VP blocks for TEM observations. In Figure 6, we note that the micelle/silica hybrid spheres with diameter of around 100 nm have much smaller central holes and, at the same time, thicker shells when compared with the morphology of the same sample after calcination. The shell thickness of the hybrid material is around 40 nm, almost twice as large as

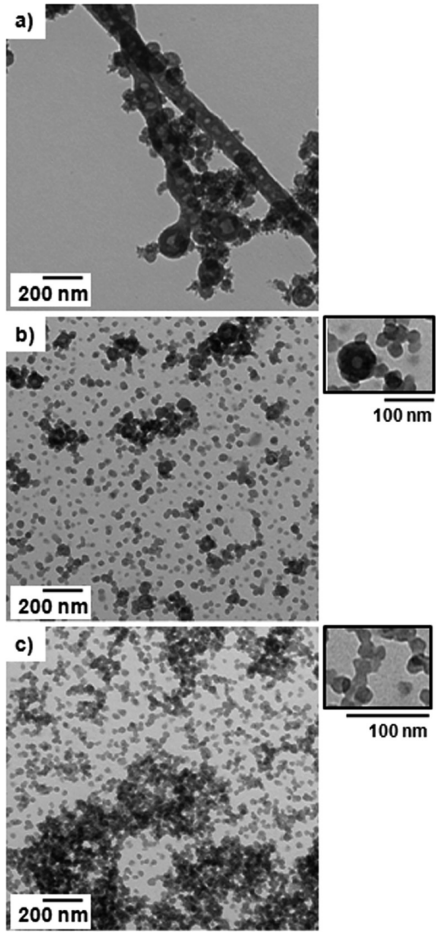

FIGURE 7. TEM images of as-synthesized silica templated by PS-*b*-P4VP with different ethanol contents in the medium. As-synthesized PS-*b*-P4VP/silica hybrids were synthesized in a mixed medium with (a) $X = 10$, (b) $X = 30$, and (c) $X = 70$ (by weight) in X:100 ethanol/water.

the shell thickness of large hollow silica spheres. The hole diameters of the micelle/silica hybrids also lie in the range 25−40 nm and they become much larger after calcination.

This experimental evidence leads us to suggest the second path in Figure 6d. As silica precursor TEOS is added, weakly cationic micelles with a few binding sites with silica precursors tend to aggregate together. Several micellar aggregates associated with silica precursors could, in turn, serve as templates for either large hollow spheres or hollow tubules. The formation of tubules is believed to originate from the connection of large spheres (i.e., path 3 in Figure 6d). We found the evidence that a tubule is formed by the aggregation of large hollow spheres, as shown in Figure 6a, and the diameters of all of the tubules are above 55 nm, much larger than the size of a single micelle. We believe that the reason why we have rather straight tubules compared with the random aggregation of large spheres is that the large micellar aggregates tend to line up during condensation of silica precursors (19). Consequently, the comparison between morphologies of as-synthesized and calcined samples leads us to the conclusion that micellar aggregates, mediated with silica precursors, are required to form both large hollow tubules and spheres.

3.3.2. Effect of Ethanol. In the experiments with different ethanol contents in water/ethanol mixtures, the major effective parameter influencing the morphological change of hollow silica is again the degree of counterion binding to positively charged P4VPs. The increase in the ethanol content effectively reduces the dielectric constant of the solution, which, in turn, enhances the Coulombic interaction between protonated P4VP chains and counterions Cl^-.

According to Coulomb's law, the electrostatic force between countercharges is proportional to the magnitudes of two charges divided by the dielectric constant of the medium and inversely proportional to the square of the distance between charges. Thus, in high ethanol content, the Coulombic interaction between protonated P4VP and Cl^- counterions becomes stronger than the case without ethanol because of the reduced dielectric constant of the medium, leading to the formation of tightly bound ion pairs. The strong attractive interaction between protonated P4VP and Cl^- counterions also influences the structure of hollow silica, which is quite similar to the cases shown with quaternized PS-*b*-P4VPs. In the presence of excess ethanol, the strong dipole−dipole interactions among P4VP chains effectively induce the physically cross-linked state within a micelle, resisting deformation of the original micellar shape or morphological change during association with the silica precursors. That is to say that the intermolecular interaction between positive polymers and negative counterions controls the morphology of hollow silica (from tubules to large hollow spheres to small hollow spheres).

The origin of the tubules, large hollow spheres, and small hollow spheres from PS-*b*-P4VPs (unquaternized) with different amounts of ethanol in the medium are also investigated by TEM on as-synthesized PS-*b*-P4VP/silica hybrids, as shown in Figure 7. At X (g of ethanol in 100 g of water) = 10, long rods with connected spheres, large hollow spheres with small holes, and small spheres in micelle size without holes coexist. As the amount of ethanol is increased to X = 70, rods and large hollow spheres disappear while small spheres in micelle size are dominantly observed, indicating the morphological change among three different phases similar to the cases observed with quaternized PS-*b*-P4VPs.

4. CONCLUSIONS

In summary, we demonstrate the morphological change from tubules to large hollow spheres to (micelle-sized) small hollow spherical silica by adjusting the intermolecular interactions within micelles: the type and density of counterions during the quaternization of P4VP chains as well as variation of the solution dielectric constant by the addition of ethanol influences the strength of the intermolecular interactions among positively charged P4VPs and counterions (Cl^- or I^-) within the micelles. The effect of dipole−dipole interactions among ion pairs for P4VP blocks (either quaternized or protonated P4VPs) and subsequent silica condensation on the final silica morphology are elucidated with a general picture including

previously reported results (showing only micelle-sized small hollow silica (8)). We believe that the approach taken in this study, the manipulation of ion-pair associations in block templates for the morphological control of hollow silica, can be applied to other systems of interest.

Acknowledgment. This work was financially supported by the Korea Science and Engineering Foundation (KOSEF) through Acceleration Research funded by the Ministry of Education, Science and Technology (MEST; Grant R17-2007-059-01000-0) and by the NANO Systems Institute through the KOSEF (Grant R15-2003-032-02002-0). We also acknowledge financial support from the MEST through the Brain Korea 21 Program and the World Class University Program (400-2008-0230) at Seoul National University. Additional financial support from the NGNT Project (No. 10024135) supported by the Ministry of Commerce, Industry and Energy is greatly acknowledged.

Supporting Information Available: Detailed information on the size distribution of hollow silica prepared in this study. This material is available free of charge via the Internet at http://pubs.acs.org.

REFERENCES AND NOTES

(1) Chen, J.; Ding, H.; Wang, J.; Shao, L. *Biomaterials* **2004**, *25*, 723–727.
(2) Li, H.; Bian, Z.; Zhu, J.; Zhang, D.; Li, G.; Huo, Y.; Li, H.; Lu, Y. *J. Am. Chem. Soc.* **2007**, *129*, 8406–8407.
(3) (a) Fujiwara, M.; Shiokawa, K.; Hayashi, K.; Morigaki, K.; Nakahara, Y. *J. Biomed. Mater. Res., Part A* **2006**, *81*, 103–111. (b) Suh, W. H.; Jang, A. R.; Suh, Y.-H.; Suslick, K. S. *Adv. Mater.* **2006**, *18*, 1832–1837.
(4) Murthy, V.; Cha, J. N.; Stucky, G. D.; Wong, M. S. *J. Am. Chem. Soc.* **2004**, *126*, 5292–5299.
(5) Li, W.; Coppens, M.-O. *Chem. Mater.* **2005**, *17*, 2241–2246.
(6) Bruinsma, P. T.; Kim, A. Y.; Liu, J.; Baskaran, S. *Chem. Mater.* **1997**, *9*, 2507–2512.
(7) Caruso, F.; Caruso, R. A.; Möhwald, H. *Science* **1998**, *282*, 1111–1114.
(8) (a) Khanal, A.; Inoue, Y.; Yada, M.; Nakashima, K. *J. Am. Chem. Soc.* **2007**, *129*, 1534–1535. (b) Yuan, J.-J.; Mykhaylyk, O.; Ryan, A.; Armes, S. *J. Am. Chem. Soc.* **2007**, *129*, 1717–1723.
(9) Huo, Q.; Margolese, D. I.; Ciesla, U.; Demuth, D. G.; Feng, P.; Gier, T. E.; Sieger, P.; Firouzi, A.; Chmelka, B. F.; Schüth, F.; Stucky, G. D. *Chem. Mater.* **1994**, *6*, 1176–1191.
(10) (a) Lin, H.-P.; Kao, C.-P.; Mou, C.-Y.; Liu, S.-B. *J. Phys. Chem. B* **2000**, *104*, 7885–7894. (b) Che, S.; Li, H.; Lim, S.; Sakamoto, S.; Terasaki, O.; Tatsumi, T. *Chem. Mater.* **2005**, *17*, 4103–4114.
(11) Atkins P. W. *Physical Chemistry*; Oxford University Press: Oxford, England, 1998; Vol. 2,Further Information 5.
(12) (a) Khokholov, A. R.; Kramarenko, E. Y. *Macromol. Theory Simul.* **1994**, *3*, 45–59. (b) Kawaguchi, D.; Satoh, M. *Macromolecules* **1999**, *32*, 7828–7835.
(13) (a) Zhu, J.; Eisenberg, A.; Lennox, R. B.; Khokholov, A. R. *J. Am. Chem. Soc.* **1991**, *113*, 5583–5588. (b) Nguyen, D.; Varsheny, S. K.; Williams, C. E.; Eisenberg, A. *Macromolecules* **1994**, *27*, 5086–5089.
(14) (a) Gauthier, S.; Duchesne, D.; Eisenberg, A. *Macromolecules* **1987**, *20*, 753–759. (b) Frederick, C.; Schwab, C.; Hellwell, I. *J. Ind. Eng. Chem. Prod. Dev.* **1984**, *23*, 435–436.
(15) Satoh, M.; Yoda, E.; Hayashi, T.; Komiyama, J. *Macromolecules* **1989**, *22*, 1808–1812.
(16) (a) Bicak, N.; Gazi, M. *J. Macromol. Sci., Part A* **2003**, *40*, 585–591. (b) Chen, D.; Peng, H.; Jiang, M. *Macromolecules* **2003**, *36*, 2576–2578.
(17) Dielectric constants of each solvent: $\epsilon_{H_2O} = 78$; $\epsilon_{ethanol} = 25$.
(18) Leontidis, E. *Curr. Opin. Colloid Interface Sci.* **2002**, *7*, 81–91.
(19) Steinberg, Y.; Schroeder, A.; Talmon, Y.; Schmidt, J.; Khalfin, R. L.; Cohen, Y.; Devoisselle, J.-M.; Begu, S.; Avnir, D. *Langmuir* **2007**, *23*, 12024–12031.

AM900026S